Received: 3 January 2020 | Revised: 11 May 2020 | Accepted: 27 May 2020

DOI: 10.1111/jace.17317

RAPID COMMUNICATION

Journal of the American Ceramic Society

CVD synthesis and characterization of thin Mo_2C crystals

Furkan Turker[1] | **Omer R. Caylan**[1] | **Naveed Mehmood**[2] | **Talip S. Kasirga**[3] | **Cem Sevik**[4] | **Goknur Cambaz Buke**[5]

[1]Micro and Nanotechnology Graduate Program, TOBB University of Economics and Technology, Ankara, Turkey

[2]UNAM, Institute of Materials Science and Nanotechnology, Bilkent University, Ankara, Turkey

[3]Department of Physics, UNAM, Institute of Materials Science and Nanotechnology, Bilkent University, Ankara, Turkey

[4]Department of Mechanical Engineering, Eskisehir Technical University, Eskisehir, Turkey

[5]Department of Materials Science and Nanotechnology Engineering; Micro and Nanotechnology Graduate Program, TOBB University of Economics and Technology, Ankara, Turkey

Correspondence
Goknur Cambaz Buke, TOBB ETU, Materials Science and Nanotechnology Eng., Sogutozu Cad., No:43, 06560, Cankaya, Ankara, Turkey.
Email: goknurcambaz@gmail.com; goknurbuke@etu.edu.tr

Funding information
Air Force Office of Scientific Research, Grant/Award Number: FA9550-19-1-7048

Abstract

In this study, we present an investigation on the growth of thin Mo_2C crystals via chemical vapor deposition using CH_4. Optical microscopy (OM), scanning electron microscopy (SEM), atomic force microscopy(AFM), and Raman spectroscopy studies show that the morphology and the thickness of Mo_2C crystals are strongly affected by the impurities in the system, the thickness of the copper substrate, and the graphene presence on Cu surface prior to Mo_2C formation. Our studies show that during the CVD process, orthorhombic Mo_2C crystals grow along the [100] direction on two different regions: directly on Cu surface or on graphene covered regions. Mo_2C crystals that form on graphene are found to be thinner and less defective compared to the ones formed on the Cu surface. This is attributed to graphene acting as an additional diffusion barrier for Mo atoms diffusing through the copper. In addition to the graphene beneath the Mo_2C crystal, Raman studies indicate that graphene may grow also on top of the Mo_2C crystal, forming a graphene/Mo_2C/graphene sandwich structure which may offer interesting properties for electronic applications.

KEYWORDS

2D Mo_2C, copper foil, CVD, graphene, impurities

1 | INTRODUCTION

Recently, 2D Mo_2C has drawn remarkable interest owing to its high strength,[1] hardness,[2] good corrosion resistance at high temperatures,[3] high chemical stability,[4] catalytic activity[5] and superconductivity[6] which make it an important candidate material for various applications such as electrochemical batteries,[7,8] supercapacitors,[9,10] electromagnetic interference shielding,[11,12] and hydrogen evaluation reactions.[5] Not only for the uses in these applications but also to study the fundamentals (eg the relationship between the morphology and properties of 2D Mo_2C at nanoscale), controlled synthesis (thickness, lateral size, defects) of these thin crystals is required.

CVD has been a promising technique to achieve large area and high quality thin layers of Mo_2C[3,13,22,14-21]. In this method, Cu foil is placed on a Mo substrate and heated. At above the melting temperature of copper, hydrocarbon gas (CH_4) is introduced into the system, so that the Mo atoms diffusing through the copper, meet carbon atoms at the surface and form Mo_2C.[3] In this process, besides the classical CVD processing parameters such as reaction temperature[23] and duration,[14] copper thickness and CH_4 flow rate play critical roles in the determination of the final Mo_2C crystal thickness.[13,14]

Firstly, Cu thickness is important because it does not only act as a catalyst, but also as a valve or membrane, controlling the Mo supply for the formation of 2D Mo_2C crystals.[13]With

respect to this, studies[13,20] agree that Mo_2C crystals get thinner with increasing thickness of Cu layer. Secondly, CH_4 flow rate is also very critical not only because it is the carbon source in Mo_2C, but also the excess amount results in the formation of graphene, which may act as an additional diffusion barrier in the supply of Mo atoms.[17] Although various groups have mentioned simultaneous growth of graphene and Mo_2C, there are conflicts in the positional relationship between graphene and Mo_2C as well as their formation mechanism.[14-17,24] For example, while Geng et al claims the evolution of graphene beneath 2D Mo_2C,[14] with similar growth conditions, Deng et al suggests the formation of graphene on top of Mo_2C crystals.[15]

In short, the effects of reaction temperature, duration, copper thickness, and CH_4 flow rate on the final morphology and thickness of Mo_2C crystals were studied to some extent, but there are discrepancies and conflicting data in literature. Furthermore, from the graphene CVD studies,[25,26] it is known that Si, originating from the quartz tube, affects the nucleation and growth behavior of graphene, but there is not any study showing the effect of impurities on the growth of Mo_2C crystals through this method. In this study, the effects of impurities in the system, copper thickness, and graphene formation on the growing Mo_2C crystal's morphology and thickness were studied systematically. The positional relationship between graphene and Mo_2C was investigated directly on Cu surface and on transferred Si surface through detailed Raman Spectroscopy studies.

2 | EXPERIMENTAL PROCEDURE

2.1 | Mo_2C synthesis

A Cu foil (Alfa Aesar, 0.025 mm thick, 99.8% purity, 5×5 mm^2) and a Mo foil (Nanografi, 0.1 mm thick, 99.5% purity, 8×8 mm^2) were pretreated by immersing the substrates in acetic acid bath (99.8%–100.5%, Sigma-Aldrich), DI water, and ethanol sequentially (10 minutes each) to remove the native oxide layer existing on the metal surface. Cu foil on top of a Mo foil was then placed in a mass flow controlled (MFC) hot-wall CVD furnace (Protherm) with a 100 cm long horizontal quartz tube (d = 8 cm). Prior to heating, the quartz chamber was first purged with argon and then pumped down to base pressure (5 mTorr) using a mechanical pump. Subsequently, the substrates were heated to 1090°C in 2 hours under 20 sccm H_2 flow. Once the furnace temperature reached 1090°C, 0.5 sccm methane flow was introduced into the reaction tube to initiate the growth while maintaining the H_2 flow at 20 sccm at ambient pressure of 700 Torr. Following the growth (30 minutes), the sample was cooled down to room temperature in 2 hours by furnace cooling. In order to investigate the effect of impurities coming from the furnace environment (eg quartz tube) the experiments were conducted with and without carbon sheet with a thickness of 35 μm (Nanografi, NG01GS0102)on top of the substrates.

2.2 | Transfer of Mo_2C crystals onto the Si/SiO_2 wafers

For the transfer of the formed crystals on the surface, PMMA layer, 200-300 nm in thickness, was first spin coated on the surface of the heterostructures at 5000 rpm for 1 minutes and cured at 150°C for 5 minutes. Subsequently, the samples were immersed in a 0.7 mol/L $(NH_4)_2S_2O_8$ solution at RT to etch Cu foil and detach the Mo_2C/PMMA stack from substrate. Then, the samples were rinsed with DI water several times to remove the etchant and Cu residues. Thereafter, PMMA-coated crystals were placed onto HF treated Si/SiO_2 wafers. Finally, the PMMA was removed by hot acetone (~50°C) to obtain free crystals on Si/SiO_2 wafers.

2.3 | Characterization

The distribution of Mo_2C crystals on Cu and their oxidation behavior were studied using optical microscopy (Nikon Eclipse LV150N). The surface morphology of Cu and graphene/Mo_2C heterostructures were identified via SEM equipped with electron dispersive spectroscopy (EDS) (FEI Quanta 200 FEG). The thicknesses of graphene/Mo_2C structures were determined through AFM in the tapping mode (Asylum MFP-30, Oxford Instruments, USA). Mo_2C formation along with graphene was confirmed using Raman spectroscopy (Witec Alpha300S with an excitation wavelength of 532 nm) and X-ray photoelectron spectroscopy (XPS) (K-Alpha Model XPS spectrometer, Thermo Fisher Scientific, UK; Al Kα radiation, 1486.6 eV was employed as the X-ray source). X-ray diffraction (XRD) was employed to determine the phase and the orientation of Mo_2C crystals (D8 Advance Bruker with Cu$K\alpha$ radiation).

2.4 | Raman off-resonant spectrum calculations

The phonon frequency calculations were performed by Density Functional Perturbation theory as implemented in the Vienna ab initio simulation package (VASP) code[27] which is based on Density Functional Theory (DFT).[28,29] The generalized gradient approximation in its PBE parameterization was used for electronic exchange-correlation functional.[30] An energy cut-off of 700 eV, and a 24X24X1 Monkhorst-Pack k-point grid was used for the plane wave expansion

and Brillouin-zone sampling respectively. The corresponding Raman off-resonant spectrum was obtained by using the derivative of a macroscopic dielectric tensor with respect to each vibrational mode at gamma point.[31]

2.5 | Device fabrication and transport measurements

Electrical characterization was performed on Mo_2C crystals transferred over the oxidized Si chips in two terminal device configurations. The electrical contacts were formed with molten indium needles. First, indium source was placed over a hotplate under the optical microscope. Once the indium melts around 160℃, a cold needle attached to a motorized micromanipulator was inserted to the liquid indium and drawn out to form the needle. Then, the substrate with the transferred crystals was placed over the hotplate and the indium needle is contacted with the target crystal. To speed up the metal contacting process, another needle was formed from the end of the placed indium needle and placed over the crystal. The total exposure of the sample to the high temperatures was limited to less than a minute. Current-Voltage (I-V) measurements were taken using a source measure unit (Keithley 2400) under the ambient conditions, immediately after the device fabrication. The crystal thickness and the device dimensions for the resistivity calculations were determined from SEM images.

Crystal structure drawings were produced by VESTA.[32]

3 | RESULTS AND DISCUSSION

In order to investigate the effect of impurities on the formation and growth mechanisms of Mo_2C crystals, the experiments were conducted with and without carbon sheet on top of the substrates (Figure 1). Studies show that if Cu was not covered by a carbon sheet, mostly equiaxed crystals with 2 μm in diameter, and columnar structures with 20 μm in length and 2 μm in width were formed. EDAX result (Figure 1G), taken from the surface of the sample (marked region in Figure 1E), shows the presence of Mo, C, Cu, Ca, Si, and O. Given that the atomic ratio of Ca, Si, and O is 1:1:3, it may indicate the formation of $CaSiO_3$ compound as a contamination on the Cucatalyst surface. Ca impurities were most probably originated from 99.8% pure Cu foil due to the frequent use of $CaCO_3$ during Cu extraction.[25]

To synthesize large area Mo_2C crystals free from contamination, carbon sheet was placed on top of Mo-Cu substrate to substantially block the Si atoms coming from the quartz tube (Figure 1B). Thereby, it was ensured that Si atoms land on top of carbon sheet rather than Cu surface and intensive formation of nucleation centers was prevented. Optical microscope and SEM images (Figure 1D,F) exhibit the evolution of flower-like crystals which are relatively large in lateral size (~15 μm). EDS studies confirm that carbon sheet successfully block the Si atoms (Figure 1H).

For the chemical analysis, flower-like crystals, shown in Figure 1D,F, were investigated using XPS. The high-resolution Mo 3d spectrum was deconvoluted into three pairs

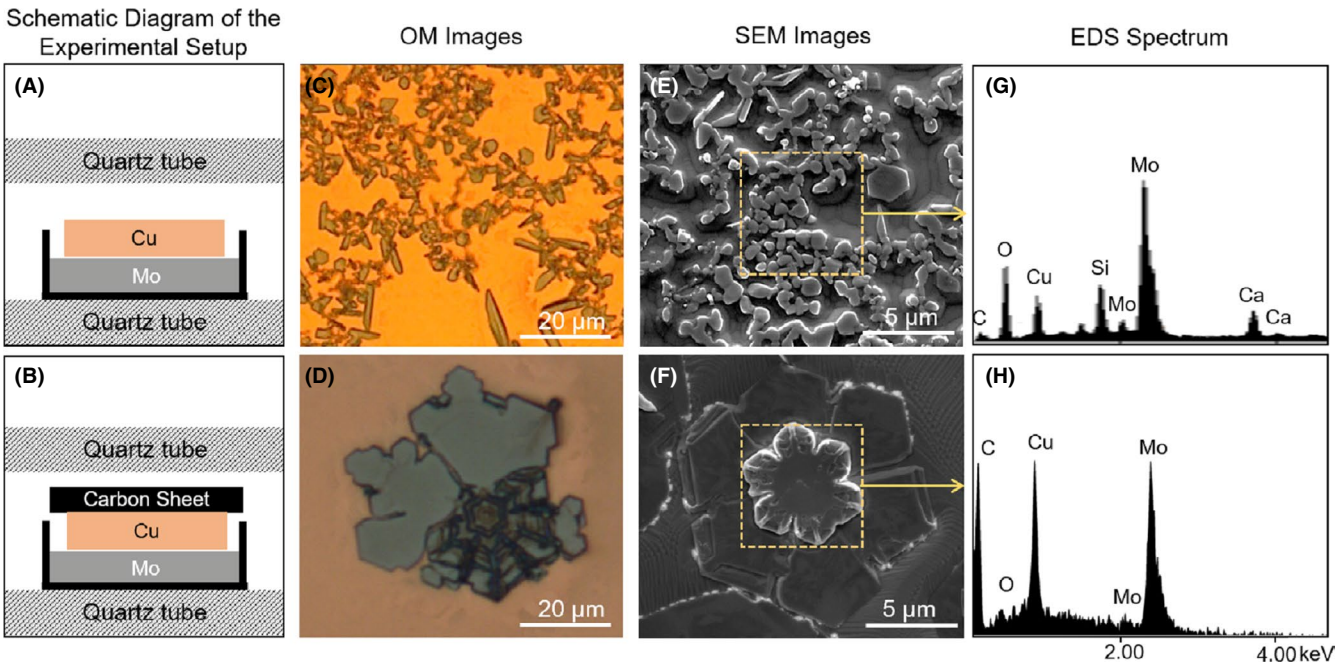

FIGURE 1 The effect of contamination on the growth of Mo_2C crystals: (A, B), Schematic representations of the experimental setup; (C, D) optical micrographs; (E, F) SEM images and (G, H) EDAX results of the samples synthesized without and with carbon sheet cap on top of Mo-Cu substrate respectively [Color figure can be viewed at wileyonlinelibrary.com]

of peaks (Figure 2A). In addition to the Mo-C peaks at 228 and 231.2 eV, the peaks at binding energies of 228.4, 232.2, 232.7, 235.5 eV are assigned to Mo^{+4} and Mo^{+6} species, which can be attributed to the surface oxidation of Mo_2C in air.[33,34] The high resolution C 1s spectra (Figure 2B) of the sample can be well-fitted into two peaks, indicating the formation of graphene (sp^2 hybridized C-C at 284.3 eV)[35] along with Mo_2C (Mo-C at 284.2 eV),[33] in line with previous works where they demonstrated the formation of graphene along with Mo_2C crystals at a high ratio of CH_4 to H_2 flow rate (≥1:60).[14-16]

In the CVD growth of Mo_2C, Cu layer acts as a valve or membrane, controlling the Mo supply for the formation of 2D Mo_2C crystals. Hence, in order to decrease the thickness and control the shape of the crystals, the supply of the Mo atoms can be decreased by increasing the Cu layer thickness. In order to test this hypothesis, various numbers of Cu foils (1, 3, and 5) were placed on top of the Mo foils, and the crystals formed at the center region of the samples were compared (Figure 3). In the case of 1 layer Cu, the formed Mo_2C crystals have flower shape morphology with thickness reaching to 200 nm (Figure 1A-D). When 3 Cu layers were used, thinner crystals with facets were observed. Furthermore, experiments performed by using 5 Cu layers resulted in the formation of very thin Mo_2C crystals (20 nm) with well-defined facets (Figure 3I-L).

The thin crystals formed by using 5 Cu foils were further analyzed through XRD. The diffraction patterns were assigned to orthorhombic Mo_2C phase[36] (Figure 4A). Moreover, from XRD analysis one can deduce that the crystals grew along the [100] direction which is in parallel with the literature.[3]

XRD results were also confirmed by the experimental and theoretical Raman Spectroscopy studies. Figure 4B shows the Raman spectrum measurement (blue solid line) for a thin-film structure exemplarily depicted in Figure 3, and off-resonant Raman spectrum (solid red lines) calculated for orthorhombic α-Mo_2C bulk crystal, along with Gamma point phonon frequency values (grey dashed lines). Theoretical and experimental results are in good agreement and confirms that grown Mo_2C crystals are orthorhombic. Both results are distinctly different from the Raman spectrum of other possible crystal formations well-known as 2H- and 1T-MoS_2, possessing three discrete Raman active modes.[37]

During the growth of Mo_2C crystals, due to the CH_4 flow at high temperature, graphene forms at the surface simultaneously. The graphene formation is critical, because it acts as an additional diffusion barrier which may help to form the thinner Mo_2C crystals by slowing down the Mo supply. In order to study this effect, detailed experiments were conducted using five Cu foils.

The graphene covered regions were revealed by oxidation experiments. The surfaces of the samples with Mo_2C crystals before and after oxidation are compared in Figure 5A,B. Upon oxidation, graphene covered Cu surface was protected from oxidation, whereas Cu regions were oxidized (dark orange regions in Figure 5B).SEM image of the selected area in Figure 5A is given in Figure 5C, where the different regions are clearly seen. These results indicate that during the CVD process, Mo_2C crystals may form on two different regions: directly on Cu surface (designated as Region 3 in Figure 5) or on graphene (designated as Region 4 in Figure 5). Furthermore, Mo_2C crystals that form on graphene were found to be thinner and less defective compared to the ones formed on the Cu surface.

To determine the positional relationship of graphene and Mo_2C crystals, Raman spectrum was collected from the designated regions in Figure 5C. Raman spectroscopy studies together with oxidation experiments confirmed that the region 1 is graphene on copper, region 2 is only copper and region 3 is Mo_2C (650 cm^{-1}) on copper. Surprisingly, the Raman spectrum taken from region 4 also shows that there is also graphene layer on Mo_2C crystal (Region 4).

In order to check whether there is graphene under the Mo_2C crystal in region 4 and to decrease the noise to signal ratio (fluorescence caused by Cu substrate), structures

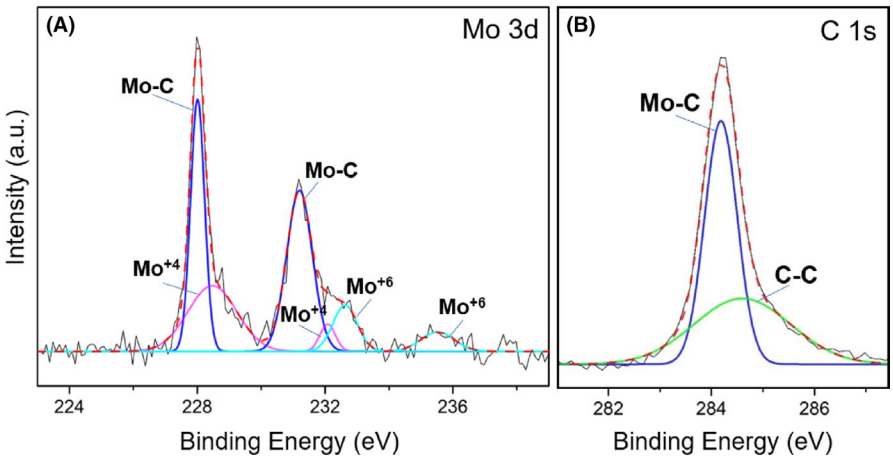

FIGURE 2 Surface chemical analysis of Mo_2C crystals through XPS. High resolution (A) Mo 3d and (B) C 1s spectra [Color figure can be viewed at wileyonlinelibrary.com]

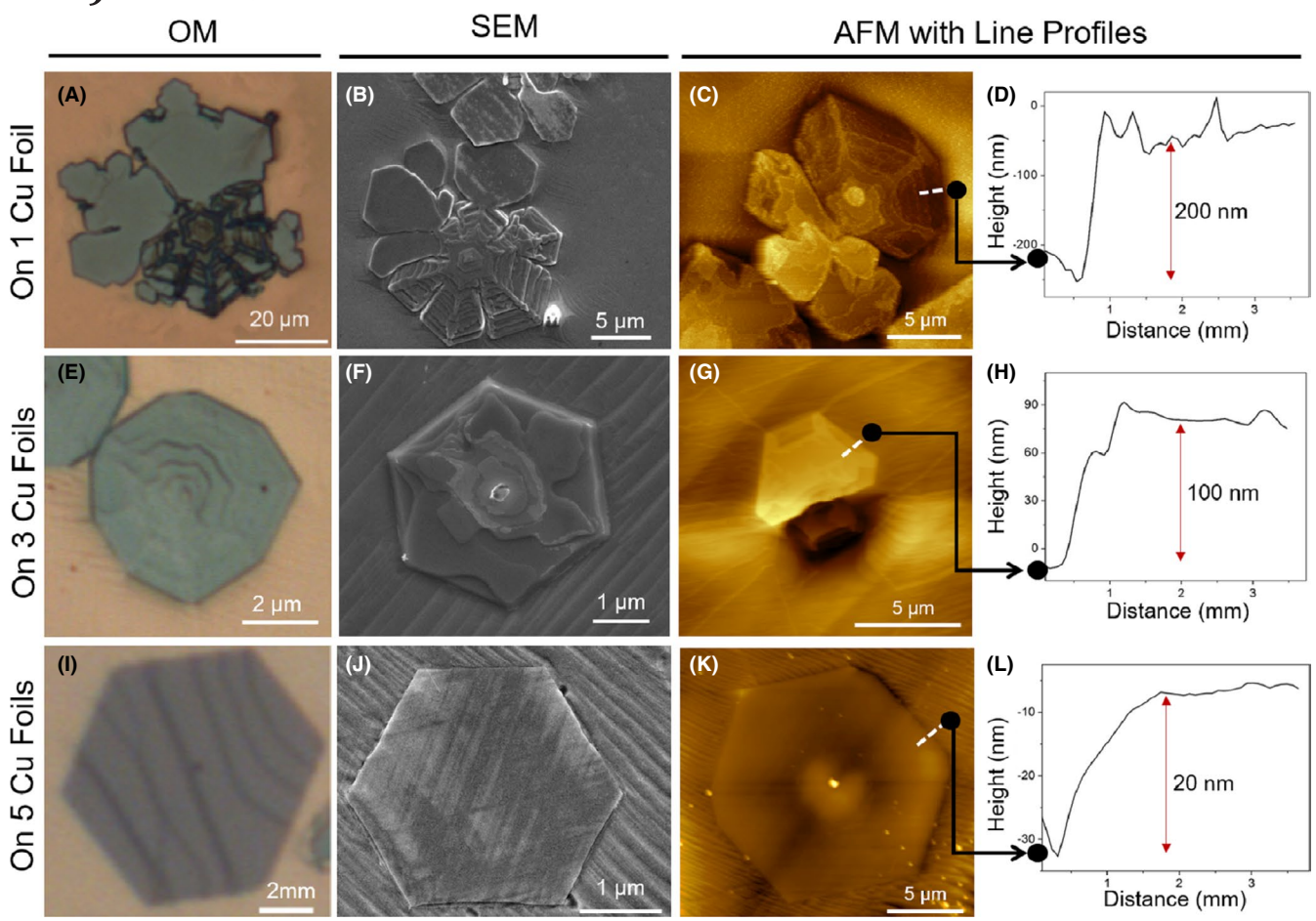

FIGURE 3 Optical microscope, SEM, AFM images, and corresponding height profiles of Mo_2C crystals grown on (A-D) one, (E-H) three, and (I-L) five copper foils [Color figure can be viewed at wileyonlinelibrary.com]

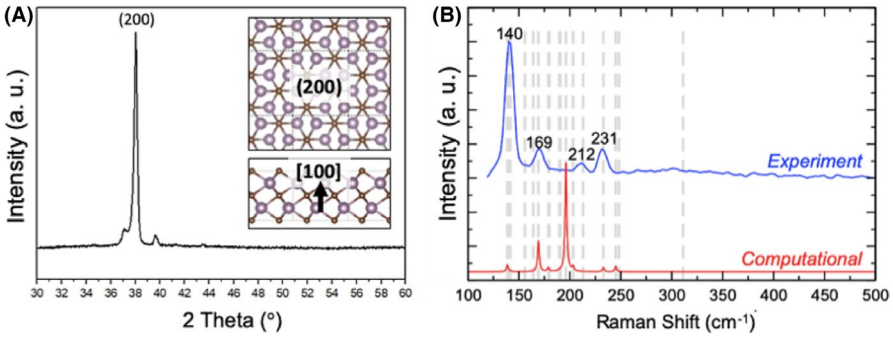

FIGURE 4 A, XRD pattern of Mo_2C domains on Cu (inset shows Mo_2C crystal's top and side view); (B) measured Raman spectrum of an as-grown thin film structure (blue line) and off-resonant Raman spectrum calculated for bulk α-Mo_2C crystal. Here, the gray dashed lines show the calculated Gamma point phonon frequencies [Color figure can be viewed at wileyonlinelibrary.com]

formed on Cu surface were transferred onto Si substrates. Figure 6A,C exhibits the typical optical microscope image of the transferred structures on Si substrate and the corresponding Raman spectra taken from the marked spots respectively. Raman spectrum taken from the rectangular crystal (A in Figure 6A) confirms the formation of Mo_2C (650 cm^{-1})/graphene (G peak at 1580 cm^{-1} and 2D peak at 2673 cm^{-1}) heterostructure. Intensity ratio of 2D peak to G peak about 2.8 and narrow symmetric 2D peak (FWHM value of 35 cm^{-1}) shows the presence of single layer grapheme.[38,39] The absence of Si peak shows that the Mo_2C crystal is thick enough that no signal is coming from beneath. Therefore, in this spectrum the graphene signal is coming from the top of the Mo_2C crystal, supporting the result given as the spectra 4 in Figure 5. The spectrum from point C in Figure 6A verifies the growth of graphene on the Cu as well, consistent with the above optical microscope results obtained by oxidation studies. In addition, we observed that some Mo_2C

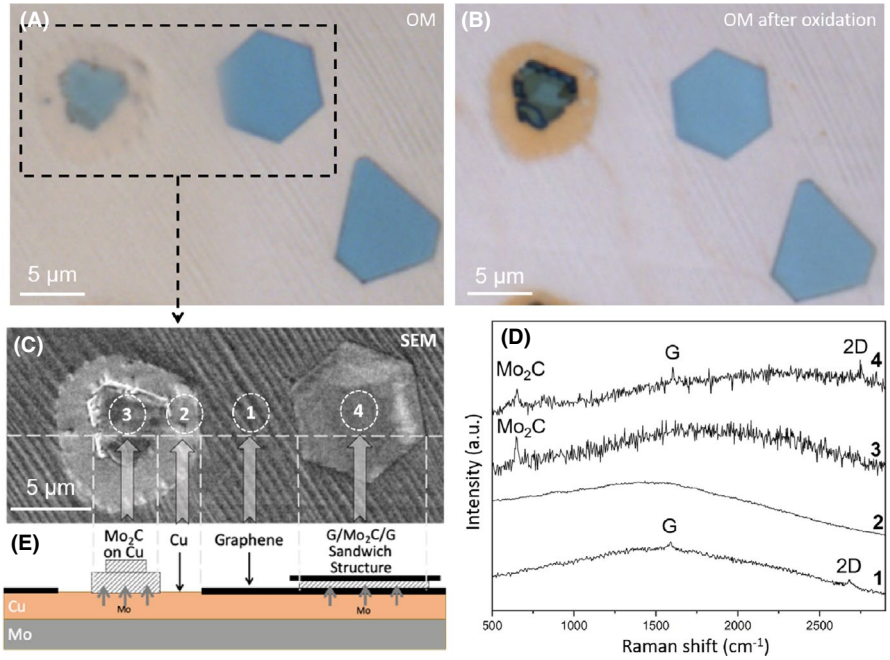

FIGURE 5 Optical micrographs of the sample surface (A) before and (B) after oxidation. Blue crystals are Mo_2C crystals; (C) SEM image of the designated region in (A); (D) Raman spectrum of the labeled regions in (C); (E) Schematic representation of the evolution of different structures on Cu surface, where the region numbers correspond to the labels in (C) [Color figure can be viewed at wileyonlinelibrary.com]

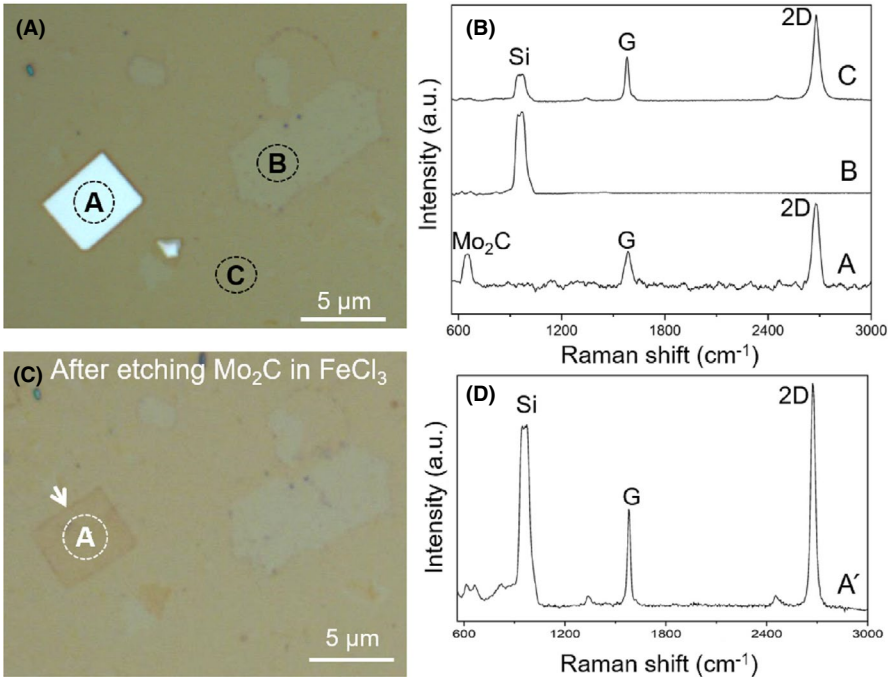

FIGURE 6 A and B, Optical micrographs and (C, D) corresponding Raman spectrums taken from the designated regions of the transferred samples (A, C) before and (B, D) after acid etching to remove the crystal from Si/SiO_2 surface [Color figure can be viewed at wileyonlinelibrary.com]

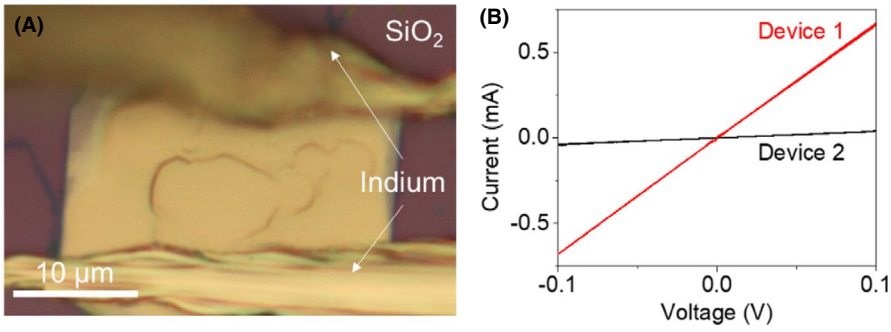

FIGURE 7 A, Optical microscope image of an indium contacted Mo_2C crystal on Si/SiO_2 substrate. B, I-V curves for two different devices of similar sample geometry [Color figure can be viewed at wileyonlinelibrary.com]

crystals fell off during the transfer process, leaving behind regular shaped edge traces (B), as presented before in Ref [19]. Raman signals collected from this region (B) shows the absence of graphene underneath the Mo_2C crystal. To answer the question if there is graphene under the rectangular Mo_2C crystal or not, the sample was etched in 1M $FeCl_3$ solution to remove the Mo_2C selectively (Figure 6B). The Raman spectroscopy studies after etching (Figure 6D) verified the presence of graphene under the crystal as well (G peak at 1595 cm^{-1} and 2D peak at 2676 cm^{-1}). This result shows that the direct growth of graphene/Mo_2C/graphene sandwich heterostructure is possible through this method.

Finally, electrical characterization of the thin Mo_2C crystals was also performed. I-V scans taken from two different devices show the Ohmic behavior of the transferred Mo_2C crystals up to 100 mV. Device 1 is shown in Figure 7A. Two I-V cycles for device 1 and 2 are given in Figure 7B. Resistivity of the device was measured to be 130×10^{-4} Ω.cm and 1200×10^{-4} Ω.cm respectively. Differences in the graphene coverage and quality of the crystals may lead to deviations in the resistivity of the samples.

4 | CONCLUSIONS

In this study, the effects of impurities, copper thickness, and graphene presence on the morphology of growing Mo_2C crystals were discussed. It was shown that Si atoms coming from the quartz tube affect the nucleation and growth behavior of Mo_2C, hence to form thin crystals with large lateral size, the surface of the sample should be covered and kept from Si deposition.

In the CVD growth of Mo_2C, Cu layer acts as a valve, controlling the Mo supply for the formation of 2D Mo_2C crystals. Our studies also confirmed that to decrease the thickness and to control the shape of the crystals further, the supply of the Mo atoms can be decreased by increasing the Cu layer thickness.

During the growth of Mo_2C crystals, due to the CH_4 flow at high temperature, graphene may form at the surface simultaneously. The graphene formation is critical, because it acts as an additional diffusion barrier which may promote the formation of thinner Mo_2C crystals.

In the light of detailed characterization studies, we showed that Mo_2C crystals, which have orthorhombic phase growing along the [100] direction, may form on two different regions: on Cu surface or on graphene. Our studies also indicated that the Mo_2C crystals that form on graphene are thinner and less defective compared to the ones formed on the Cu surface. This was attributed to the presence of graphene which acts as an additional diffusion barrier for Mo atoms coming from the bulk of copper. Furthermore, we showed that Mo_2C formed on graphene was also covered with graphene forming graphene/Mo_2C/graphene sandwich structure. To our best knowledge direct growth of graphene/Mo_2C/graphene sandwich structure is shown for the first time through this method and this heterostructure may be interesting for advanced electronic applications.

ACKNOWLEDGMENT

This material is based upon work supported by the Air Force Office of Scientific Research under award number FA9550-19-1-7048.

ORCID

Naveed Mehmood https://orcid.org/0000-0002-1278-5875
Goknur Cambaz Buke https://orcid.org/0000-0001-9587-519X

REFERENCES

1. Anasori B, Lukatskaya MR, Gogotsi Y. 2D metal carbides and nitrides (MXenes) for energy storage. Nat Rev Mater. 2017;2(2):16098.
2. Williams WS. Transition-metal carbides. Prog Solid State Chem. 1971;6(57):57–118.
3. Xu C, Wang L, Liu Z, Chen L, Guo J, Kang N, et al. Large-area high-quality 2D ultrathin Mo_2C superconducting crystals. Nat Mater. 2015;14(11):1135–41.
4. Xiao Y, Hwang JY, Sun YK. Transition metal carbide-based materials: synthesis and applications in electrochemical energy storage. J Mater Chem A. 2016;4(27):10379–93.
5. Liu Y, Yu G, Li GD, Sun Y, Asefa T, Chen W, et al. Coupling Mo_2C with Nitrogen-rich nanocarbon leads to efficient hydrogen-evolution electrocatalytic sites. Angew Chemie - Int Ed. 2015;54(37):10752–7.
6. Willens RH, Buehler E, Matthias BT. Superconductivity of the transition-metal carbides. Phys Rev. 1967;159(2):327–30.
7. Naguib M, Halim J, Lu J, Cook KM, Hultman L, Gogotsi Y, et al. New two-dimensional niobium and vanadium carbides as promising materials for Li-ion batteries. J Am Chem Soc. 2013;135(43):15966–9.
8. Er D, Li J, Naguib M, Gogotsi Y, Shenoy VB. Ti_3C_2 MXene as a high capacity electrode material for metal (Li, Na, K, Ca) ion batteries. ACS Appl Mater Interfaces. 2014;6(14):11173–9.
9. Peng Y-Y, Akuzum B, Kurra N, Zhao M-Q, Alhabeb M, Anasori B, et al. All-MXene (2D titanium carbide) solid-state microsupercapacitors for on-chip energy storage. Energy Environ Sci. 2016;9(9):2847–54.
10. Ling Z, Ren CE, Zhao M-Q, Yang J, Giammarco JM, Qiu J, et al. Flexible and conductive MXene films and nanocomposites with high capacitance. Proc Natl Acad Sci. 2014;111(47):16676–81.
11. Shahzad F, Alhabeb M, Hatter CB, Anasori B, Man Hong S, Koo CM, et al. Electromagnetic interference shielding with 2D transition metal carbides (MXenes). Science. 2016;353(6304):1137–40.
12. Liu JI, Zhang H-B, Sun R, Liu Y, Liu Z, Zhou A, et al. Hydrophobic, flexible, and lightweight MXene foams for high-performance electromagnetic-interference shielding. Adv Mater. 2017;29(38):1–6.
13. Geng D, Zhao X, Li L, Song P, Tian B, Liu W, et al. Controlled growth of ultrathin Mo_2C superconducting crystals on liquid. Cu surface. 2016;4(1);011012.
14. Geng D, Zhao X, Chen Z, Sun W, Fu W, Chen J, et al. Direct synthesis of large-area 2D Mo_2C on in situ grown graphene. Adv Mater. 2017;29(35):1–8.

15. Deng R, Zhang H, Zhang Y, Chen Z, Sui Y, Ge X, et al. Graphene/Mo_2C heterostructure directly grown by chemical vapor deposition. Chinese Phys B. 2017;26(6):1–5.
16. Qiao JB, Gong Y, Zuo WJ, Wei Y-C, Ma D-L, Yang H, et al. One-step synthesis of Van der Waals heterostructures of graphene and two-dimensional superconducting α-Mo_2C. Phys Rev B. 2017;95(20):1–6.
17. Chaitoglou S, Tsipas P, Speliotis T, Kordas G, Vavouliotis A, Dimoulas A. Insight and control of the chemical vapor deposition growth parameters and morphological characteristics of graphene/Mo_2C heterostructures over liquid catalyst. J Cryst Growth. 2018;495:46–53.
18. Chaitoglou S, Giannakopoulou T, Speliotis T, Vavouliotis A, Trapalis C, Dimoulas A. Mo_2C/graphene heterostructures: low temperature chemical vapor deposition on liquid bimetallic Sn-Cu and hydrogen evolution reaction electrocatalytic properties. Nanotechnology. 2019;30(12).
19. Li T, Luo W, Kitadai H, Wang X, Ling X. Probing the domain architecture in 2D α-Mo_2C via polarized raman spectroscopy. Adv Mater. 2019;31(8):1–9.
20. Kang Z, Zheng Z, Wei H, Zhang Z, Tan X, Xiong L, et al. Controlled growth of an Mo_2C-graphene hybrid film as an electrode in self-powered two-sided Mo_2C-graphene/$Sb_2S_{0.42}$ $Se_{2.58}$/TiO_2 photodetectors. Sensors. 2019;19(5):1–11.
21. Li L, Gao M, Shi D. Concentric advancing front corrugations and multiple ordered growth of 2D Mo_2C crystals. Cryst Growth Des. 2019;19(6):3097–102.
22. Sun W, Wang X, Feng J, Li T, Huan Y, Qiao J, et al. Controlled synthesis of 2D Mo_2C/graphene heterostructure on liquid Au substrates as enhanced electrocatalytic electrodes. J Nanotechnol. 2019;30(38):385601.
23. Nakaso K, Okuyama K, Shimada M, Pratsinis SE. Effect of reaction temperature on CVD-made TiO_2 primary particle diameter. Chem Eng Sci. 2003;58(15):3327–35.
24. Xu C, Song S, Liu Z, Chen L, Wang L, Fan D, et al. Strongly coupled high-quality graphene/2D superconducting Mo_2C vertical heterostructures with aligned orientation. ACS Nano. 2017;11(6):5906–14.
25. Senyildiz D, Ogurtani OT, Cambaz BG. The effects of acid pretreatment and surface stresses on the evolution of impurity clusters and graphene formation on Cu foil. Appl Surf Sci. 2017;425:873–8.
26. Lisi N, Dikonimos T, Buonocore F, Pittori M, Mazzaro R, Rizzoli R, et al. Contamination-free graphene by chemical vapor deposition in quartz furnaces. Sci Rep. 2017;7(1):1–11.
27. Kresse G, Furthmu J. Efficient iterative schemes for ab initio total-energy calculations using a plane-wave basis set. Phy Rev B. 1996;54(16):169–85.
28. Kohn W, Sham LJ. Self-consistent equations including exchange and correlation effects. Phys Rev. 1965;140(4A):1134–8.
29. Hohenberg P, Kohn W. Inhomogeneous electron gas. Phys Rev. 1964;136(3B):864–71.
30. Perdew JP, Burke K, Ernzerhof M. Generalized Gradient Approximation Made Simple. Phys Rev Lett. 1996;77(18):3865–8.
31. Fonari A, Stauffer S. vasp_raman.py. https://github.com/raman-sc/VASP/. 2013.
32. Momma K, Izumi F. VESTA 3 for three-dimensional visualization of crystal, volumetric and morphology data. J Appl Cryst. 2011;44:1272–6.
33. Anandan C, Mohan L, Babu PD. Electrochemical studies and growth of apatite on molybdenum doped DLC coatings on titanium alloy. Appl Surf Sci. 2014;296:86–94.
34. Wei H, Xi Q, Chen Xi'an, Guo D, Ding F, Yang Z, et al. Molybdenum carbide nanoparticles coated into the graphene wrapping N-doped porous carbon microspheres for highly efficient electrocatalytic hydrogen evolution both in acidic and alkaline media. Adv Sci. 2018;5(3):1–7.
35. Paolicelli G, Ferrer S, Comin F. Separation of the sp^3 and sp^2 components in the C1s photoemission spectra of amorphous carbon films. Phys Rev B. 1996;54(11):8064–9.
36. Dai W, Lu L, Han Y, Wang L, Wang J, Hu J, et al. Facile synthesis of Mo_2C nanoparticles from waste polyvinyl chloride. ACS Omega. 2019;4(3):4896–900.
37. Gupta U, Naidu BS, Maitra U, Singh A, Shirodkar SN, Waghmare UV, et al. Characterization of few-layer 1T-$MoSe_2$ and its superior performance in the visible-light induced hydrogen evolution reaction. APL Mater. 2014;2:092802.
38. Bhaviripudi S, Jia X, Dresselhaus MS, Kong J. Role of kinetic factors in chemical vapor deposition synthesis of uniform large area graphene using copper catalyst. Nano Lett. 2010;10(10):4128–33.
39. Reina A, Jia X, Ho J, Nezich D, Son H, Bulovic V, et al. Large area, few-layer graphene films on arbitrary substrates by chemical vapor deposition. Nano Lett. 2009;9(8):30–5.

How to cite this article: Turker F, Caylan OR, Mehmood N, Kasirga TS, Sevik C, Cambaz Buke G. CVD synthesis and characterization of thin Mo_2C crystals. *J Am Ceram Soc*. 2020;103:5586–5593. https://doi.org/10.1111/jace.17317